Turbo Detection for Mobile MIMO Underwater Acoustic Communications

Jun Tao[†], Yahong Rosa Zheng[§], Chengshan Xiao[§]

[†]Dept. of Electrical & Computer Eng., University of Missouri, Columbia, MO 65211, USA

[§]Dept. of Electrical & Computer Eng., Missouri University of Science & Technology, Rolla, MO 65409, USA

Abstract— **Turbo detection for mobile transceivers is proposed for high data-rate single-carrier multiple-input, multiple-output (MIMO) underwater acoustic (UWA) communications. The proposed detection scheme employs a MIMO Doppler preprocessor and a low-complexity MIMO turbo linear equalizer (LE). The Doppler preprocessor estimates the motion-induced Doppler shift and compensates it via symbol resampling. The preprocessed signal is then detected by the MIMO turbo LE that utilizes soft-decision minimum mean square error (MMSE) linear equalization with maximum *a posteriori* probability (MAP) channel decoding, thus improving the detection performance iteratively while maintaining low complexity. The proposed turbo detection scheme has been tested by field trial data collected by the SPACE08 experiment near Martha's Vineyard, Edgartown, MA, in 2008. Excellent detection results are achieved for 2-by-8 MIMO with mobile speed around 3 knots.**

I. Introduction

Mobile multiple-input multiple-output (MIMO) underwater acoustic (UWA) communications is challenging for several reasons: first, the delay spread of the channel is extensively long causing severe inter-symbol interference (ISI); second, the temporal variation of the MIMO channel is very fast demanding robust channel estimation and tracking; third, the mobility-caused Doppler effect is significant incurring carrier frequency offset (CFO) and compression or dilation of the received signal packets. Last, the multiplexing interference (MI) among concurrent transmission streams makes the detection even more difficult.

Many interesting approaches have been proposed for UWA receiver designs. Traditional non-iterative detection schemes have been used in [1]–[5]. The advent of turbo equalization technology has enabled powerful receiver design [6]. It has been demonstrated that turbo detection greatly improves the bit error rate (BER) performance compared to conventional non-iterative detection schemes. The iterative equalization for UWA communications has been first proposed in [7] using a joint maximum *a posteriori* probability (MAP) soft-decision equalizer and decoder. The complexity of MAP equalizer, however, is prohibitively high especially with UWA channels. Several low-complexity turbo equalization schemes have thus been adopted. In [8], the turbo decision-feedback equalizer (DFE) has been proposed and tested by a multichannel UWA transmission. In [9], the turbo DFE has been used for MIMO UWA detection. In [10], turbo block decision-feedback equalizer (BDFE) has also been proposed for MIMO UWA detection. Turbo linear equalization has also been applied to UWA communications [11], [12] with good experimental results. Recently, turbo detection for MIMO orthogonal frequency-division multiple (OFDM) systems has also been proposed in [13].

In this paper, we investigate the turbo detection for mobile MIMO UWA communications. Compared to the radio frequency (RF) mobile communication, UWA mobile transmission is much more challenging due to high Doppler to carrier frequency ratio, which could be on the order of 10^{-4} to 10^{-3}, compared to 10^{-8} to 10^{-6} for a radio channel. In this case, the Doppler estimation has to be accurate since small Doppler estimation error could cause nonnegligible residual CFO. On the other hand, the received signal waveform is either compressed or dilated due to the high motion velocity to sound speed (∼1500 m/s in water) ratio. As a result, resampling is required to achieve symbol synchronization. The proposed scheme includes a Doppler preprocessing module to combat the Doppler-induced distortion effect in the received signal, and a MIMO turbo equalization module consists of a low-complexity soft-decision MIMO linear equalizer (LE) and N MAP channel decoders, each for one transmitted stream. The proposed scheme is tested by experimental data collected at the Martha's Vineyard, Edgartown, MA, in October 2008, with satisfactory detection performance.

II. System Model

Consider a MIMO UWA system with N transducers and M hydrophones. On the transmitter side, information bit streams $\{a_{n,k}\}_{n=1}^{N}$ are independently encoded, interleaved, modulated and then transmitted by the N transducers, where k is the time index. At the n-th stream, the outputs of the encoder, the interleaver and the modulator are denoted by $b_{n,k}$, $c_{n,k}$, and $s_{n,k}$, respectively. For a Q-ary modulation with the constellation set $\mathcal{S} = \{\chi_q\}_{q=1}^{Q}$, the modulator maps every $\log_2 Q$ bits, $\{c_{n,(k-1)\log_2 Q+p}\}_{p=1}^{\log_2 Q}$, onto to one single modulation symbol $s_{n,k}$.

The baseband signal received at the m-th hydrophone is expressed by

$$y_{m,k} = \sum_{n=1}^{N} \sum_{l=0}^{L-1} h_{m,n}(k,l) s_{n,k-l} + v_{m,k} \tag{1}$$

where $h_{m,n}(k,l)$ is the l-th time-variant channel tap between the n-th transducer and the m-th hydrophone at time k.

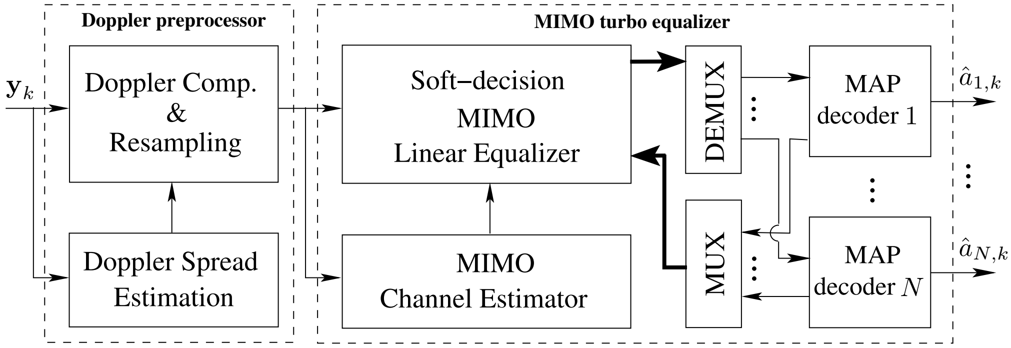

Fig. 1. Turbo detection scheme for mobile MIMO UWA communications

Stacking $\{y_{m,k}\}_{m=1}^{M}$ of all hydrophones in a vector, results in $\mathbf{y}_k = [y_{1,k}, y_{2,k}, \cdots, y_{M,k}]^t \in \mathcal{C}^{M\times 1}$ which is expressed as

$$\mathbf{y}_k = \sum_{l=0}^{L-1} \mathbf{H}_{k,l}\mathbf{s}_{k-l} + \mathbf{v}_k \tag{2}$$

where

$$\mathbf{H}_{k,l} = \begin{bmatrix} h_{1,1}(k,l) & \cdots & h_{1,N}(k,l) \\ \vdots & \ddots & \vdots \\ h_{M,1}(k,l) & \cdots & h_{M,N}(k,l) \end{bmatrix} \in \mathcal{C}^{M\times N} \tag{3}$$

$$\mathbf{s}_{k-l} = [s_{1,k-l}, s_{2,k-l}, \cdot\cdot\cdot, s_{N,k-l}]^t \in \mathcal{C}^{N\times 1} \tag{4}$$

$$\mathbf{v}_k = [v_{1,k}, v_{2,k}, \cdots, v_{M,k}]^t \in \mathcal{C}^{M\times 1} \tag{5}$$

with $(\cdot)^t$ denoting the transpose operation. The received signal $\mathbf{y}_k$ is used for detection of the transmitted symbols.

III. Proposed Detection Scheme

The block diagram of the proposed detection scheme is shown in Fig. 1, which consists of the Doppler preprocessing module and the MIMO turbo equalization module. The two modules are discussed, respectively, in the following two subsections.

A. Doppler Preprocessing

The Doppler preprocessor includes two submodules: Doppler estimation module and Doppler compensation and resampling module. Here, the Doppler estimation algorithm proposed in [14] for single-input single-output (SISO) is extended to MIMO via time-division multiplexing. Denote $f_d^{(m,n)}$ as the Doppler of the channel between the n-th transducer and the m-th hydrophone. The Doppler is related with the carrier frequency as

$$f_d^{(m,n)} = \frac{v\cdot\cos(\theta_{m,n})}{c} f_c \tag{6}$$

where v is the relative velocity between the transmitter and the receiver, c is the speed of sound propagation in water, f_c is the carrier frequency and $\theta_{m,n}$ denotes the angle between the n-th transducer's forward velocity and the line of sight from that transducer to the m-th hydrophone. Based on (6), the Doppler estimation, $\hat{f}_d^{(m,n)}$, is obtained as [14]

$$\hat{f}_d^{(m,n)} = (1 - \frac{T_{m,n}}{T}) f_c \tag{7}$$

where $T_{m,n}$ is the time duration of a packet transmitted from the n-th transducer and measured at the m-th hydrophone, T is the original time duration of the transmitted packet. When $T_{m,n} > T$, the transmitted signal is dilated. Otherwise, it is compressed. In (7), the ratio $T_{m,n}/T$ as a measurement of the degree of compression or dilation, is utilized for Doppler estimation. Finally, the measurement of the time duration of a received packet can be obtained with specifically designed signalling located at the head and tail of the packet, as will be evident in Section IV. With the estimated Doppler $\hat{f}_d^{(m,n)}$, the estimation of the corresponding resampling frequency $\hat{f}_s^{(m,n)}$ can then be calculated as

$$\hat{f}_s^{(m,n)} = \frac{f_c}{f_c - \hat{f}_d^{(m,n)}} f_s \tag{8}$$

where f_s is the sampling rate matching to the original symbol rate at the receiver side.

When the size of the transceiver platform is much smaller compared to the transmission distance, the difference among $f_d^{(m,n)}$'s for $1 \le m \le M, 1 \le n \le N$ are small since the difference among $\theta_{m,n}$'s are small. Accordingly, the signal waveforms from different transducers undergo almost the same degree of compression or dilation on the receive hydrophones. In this case, one single Doppler estimation $\hat{f}_d^{(m)}$ and one single resampling frequency estimation $\hat{f}_s^{(m)}$ can be used on the m-th hydrophone for Doppler compensation and resampling. The single Doppler estimation $\hat{f}_d^{(m)}$ and the corresponding resampling frequency estimation $\hat{f}_s^{(m)}$ can be obtained as the average of all individual Doppler estimation $\hat{f}_d^{(m,n)}$'s for $1 \le n \le N$ as

$$\hat{f}_d^{(m)} = \frac{1}{N}\sum_{n=1}^{N} \hat{f}_d^{(m,n)} \tag{9}$$

and

$$\hat{f}_s^{(m)} = \frac{f_c}{f_c - \hat{f}_d^{(m)}} f_s \tag{10}$$

The Doppler is compensated by multiplying the received signal by $e^{-j2\pi\hat{f}_d^{(m)}t}$, and the resampling of the received signal is then performed with $\hat{f}_s^{(m)}$. The same procedure is applied to all M hydrophones to obtain the preprocessed signals for detection.

B. MIMO Turbo Equalization

From Fig. 1, the MIMO turbo equalization module consists of the MIMO channel estimator, soft-decision MIMO linear equalizer together with N MAP channel decoders each for one transmitted stream. Assuming the MIMO channel remains constant over a short period of time, the channel estimation is achieved by using the pilot symbols and the previously detected symbols in the training mode and decision-directed (DD) mode, respectively [5]. With the channel knowledge, turbo detection can then be performed.

The soft-decision MIMO linear equalizer can be designed by generalizing the turbo equalization method proposed in [15] for SISO systems to the MIMO cases. In the MIMO case, the equalization of the symbol from the n-th transducer at time k relies on the received vector $\mathbf{r}_k \in \mathcal{C}^{M(K_1+K_2+1)\times 1}$ defined as

$$\begin{aligned}\mathbf{r}_k &= \left[\mathbf{y}^t_{k-K_2}, \mathbf{y}^t_{k-K_2+1}, \cdots, \mathbf{y}^t_{k+K_1}\right]^t \\ &= \mathbf{H}\mathbf{x}_k + \mathbf{z}_k \end{aligned} \tag{11}$$

where the channel matrix $\mathbf{H} \in \mathcal{C}^{M(K_1+K_2+1)\times N(K_1+K_2+L)}$, is given by

$$\mathbf{H} = \begin{bmatrix} \mathbf{H}_{L-1} & \cdots & \mathbf{H}_0 & \mathbf{0} \\ & \ddots & \ddots & \\ \mathbf{0} & \mathbf{H}_{L-1} & \cdots & \mathbf{H}_0 \end{bmatrix} \tag{12}$$

and $\mathbf{x}_k \in \mathcal{C}^{N(K_1+K_2+L)\times 1}$ and $\mathbf{z}_k \in \mathcal{C}^{M(K_1+K_2+1)\times 1}$ are denoted as

$$\mathbf{x}_k = \left[\mathbf{s}^t_{k-K_2-L+1}, \cdots, \mathbf{s}^t_{k+K_1}\right]^t \tag{13}$$

$$\mathbf{z}_k = \left[\mathbf{v}^t_{k-K_2}, \cdots, \mathbf{v}^t_{k+K_1}\right]^t \tag{14}$$

In (12), $\mathbf{H}_{k,l}$ given in (3) has been replaced by $\mathbf{H}_l$ by dropping the time index k, based on the assumption that the channel remains constant over $[k-K_2, k+K_1]$.

The equalized symbol is expressed as

$$\hat{s}_{n,k} = \mathbf{c}^h_{n,k}\tilde{\mathbf{r}}_{n,k} \tag{15}$$

where

$$\tilde{\mathbf{r}}_{n,k} = \mathbf{r}_k - \mathbf{H}\bar{\mathbf{x}}_{n,k} \tag{16}$$

and

$$\bar{\mathbf{x}}_{n,k} = \left[\bar{\mathbf{s}}^t_{k-K_2-L+1}, \cdots, \bar{\mathbf{s}}^t_{k+K_1}\right]^t \tag{17}$$

with $\bar{\mathbf{s}}_{k+l} = [\bar{s}_{1,k+l}, \cdots, \bar{s}_{N,k+l}]$ when $l \neq 0$ and $\bar{\mathbf{s}}_{k+l} = [\bar{s}_{1,k+l}, \cdots, 0, \cdots, \bar{s}_{N,k+l}]$ when $l = 0$ with the n-th element being zero. The symbol *a priori* mean $\bar{s}_{n,k}$ (and the symbol *a priori* variance $\sigma^2_{n,k}$) is calculated based on the symbol *a priori* probabilities $\{P(s_{n,k} = \chi_q)\}_{q=1}^{Q}$, which are set as $\{P(s_{n,k} = \chi_q) = \frac{1}{Q}\}_{q=1}^{Q}$ in the first iteration of the turbo equalization and are then calculated with the log-likelihood ratio (LLR) information fedback from the MAP decoders [15].

The instantaneous equalizer vector in (15) designed with minimum mean square error (MMSE) criteria, is given by

$$\begin{aligned}\mathbf{c}_{n,k} &= \mathbb{E}\left[\tilde{\mathbf{r}}_{n,k}\tilde{\mathbf{r}}^h_{n,k}\right]^{-1}\mathbb{E}\left[s^*_{n,k}\tilde{\mathbf{r}}_{n,k}\right] \\ &= [\mathbf{\Sigma}_k + (1-\sigma^2_{n,k})\mathbf{H}_n\mathbf{H}^h_n]^{-1}\mathbf{H}_n \end{aligned} \tag{18}$$

where

$$\begin{aligned}\mathbf{\Sigma}_k &\triangleq \mathrm{Cov}[\mathbf{r}(k), \mathbf{r}(k)] \\ &= \mathbf{H}\mathrm{diag}\{\sigma^2_{1,k-K_2-L+1}, \cdots, \sigma^2_{N,k-K_2-L+1}, \cdots, \sigma^2_{1,k}, \\ &\quad \cdots, \sigma^2_{N,k}, \cdots, \sigma^2_{1,k+K_1}, \cdots, \sigma^2_{N,k+K_1}\}\mathbf{H}^h + \sigma^2_v\mathbf{I} \end{aligned} \tag{19}$$

with $\mathbf{I}$ being an identity matrix of size $N(K_1+K_2+1)$, $\mathbf{H}_n$ being the $[N(K_2+L-1)+n]$-th column of $\mathbf{H}$, diag$\{\cdot\}$ returning a diagonal matrix, and Cov$[\cdot]$ calculating vector auto-covariance. In practice, it is desirable to adopt low-complexity solution for the equalizer, which is given as

$$\bar{\mathbf{c}}_n = \left\{\frac{1}{N_b}\sum_{k=1}^{N_b}\left[\mathbf{\Sigma}_k + (1-\sigma^2_{n,k})\mathbf{H}_n\mathbf{H}^h_n\right]\right\}^{-1}\mathbf{H}_n \tag{20}$$

for a sequence length of N_b. The mechanism of turbo equalization and the details on the calculations and exchanges of the LLR between the soft-decision MIMO LE and the MAP decoders are referred to [15]. In the last iteration, the turbo equalization module outputs the hard decisions $\{\hat{a}_{n,k}\}_{n=1}^{N}$ of the N transmitted bit streams.

IV. Experimental Results

Single carrier MIMO underwater acoustic experiments were conducted at the coast of Martha's Vineyard, Edgartown, MA, in October 2008. The transmission rate was 9.7656 kilo symbols per second (ksps), and the carrier frequency was 13 kHz. The QPSK, 8PSK, 16QAM and 64QAM modulation schemes were used. The transmit platform consisting of four transducers was fixed in the water, while the receive platform consisting of eight hydrophones was towed at a maximum speed of 3 knots. The transmission distance ranged from 400 to 1500 meters.

The transmission streams were organized in packets with the structure of a packet for the n-th transducer shown in Fig. 2. From the figure, two linear frequency modulation (LFM) signals named LFMB and LFME are placed at the beginning and end of the packet, respectively. The LFM signals, which have good correlation property, can be used to locate the start and end of the packet at the receiver by detecting two correlation peaks. It is shown that the structure design guarantees that LFM signals from different transducers doesn't overlap in time so that independent correlation peaks can be detected for each transducer-hydrophone pair (n, m). The two correlation peaks of LFMB and LFME for the transducer-hydrophone pair (n, m) are used to measure the time duration $T_{m,n}$ of the received packet. With $T_{m,n}$, Doppler estimation $\hat{f}_d^{(m,n)}$ can be calculated according to (7). In the packet, *m*-sequence is also embedded. The *m*-sequence can be

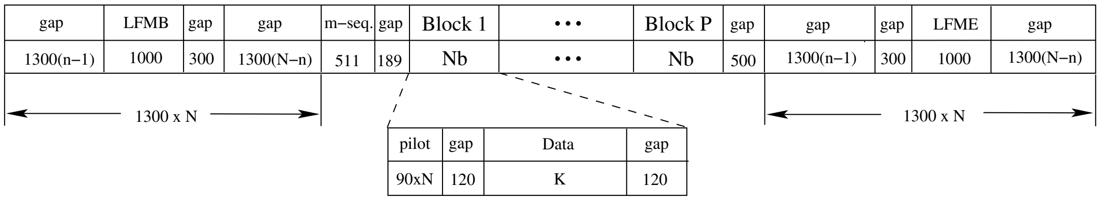

Fig. 2. Structure of transmitted packet from the n-th transducer

TABLE I
DOPPLER ESTIMATION FOR 2×8 MIMO TRANSMISSION (HZ)

n \ m	1	2	3	4
1	-18.52	-18.48	-18.15	-18.43
2	-18.34	-18.43	-18.48	-18.43
n \ m	**5**	**6**	**7**	**8**
1	-18.38	-18.19	-18.44	-18.38
2	-18.43	-18.57	-18.52	-18.38

used to evaluate the channel *scattering function*, as a function of the delay spread and the Doppler spread. The reason for choosing *m*-sequence is due to its sensitivity to Doppler. The data in the packet is organized into P blocks with each block independently encoded, randomly interleaved, and modulated before transmission. Each block starts with a pilot subblock followed by K symbols with K having three choices of 1024, 2048 and 4096. The P blocks repeat for each of the four modulation schemes.

An example of Doppler estimation is shown in Table I. From the table, it is obvious the estimated Doppler $\hat{f}_d^{(m,n)}$ are close to each other as expected. The visual demonstration of the Doppler effect resorts to the channel scattering function, as shown in Fig. 3. From the figure, the Doppler spectrum is centered around -18 Hz, incurring a Doppler to carrier frequency ratio of 1.385×10^{-3} in contrast to 10^{-9} to 10^{-7} for a radio channel. It is noted that the center Doppler (Doppler shift) in the figure matches that given by Table I.

With proper Doppler compensation and resampling operation, the received baseband signal is ready to be detected. The channel length is found to be $L = 80$ for this experiment based on the span of LFM correlation. For each transmission block, the initial channel estimation is obtained with the pilot symbols in front of it. As an example, the estimated MIMO channel for a 2×8 MIMO transmission is shown in Fig. 4.

We have processed the packets for 2×8 MIMO transmission. For the choice of block size $K = 1024$, there are $P = 10$ blocks for each modulation scheme in each packet. In Fig. 5, the soft-decision symbols at the output of the soft-decision MIMO LE and the MAP decoders are plotted for QPSK modulation. The effectiveness of the iterative processing is clearly demonstrated and all symbols are properly classified after the first iteration. The detection results for two packets are listed in Table II. It is obvious that for all but one blocks,

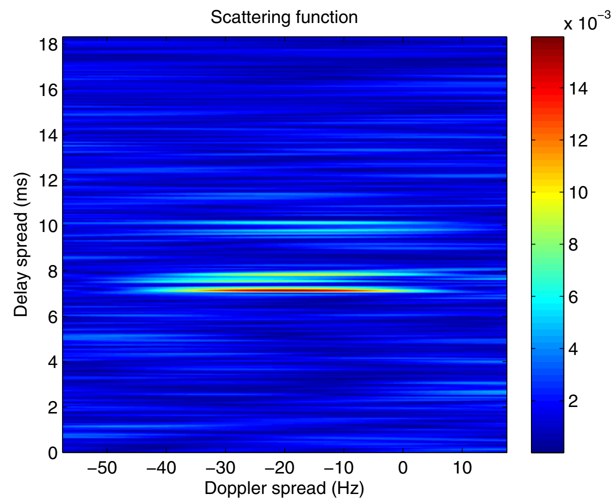

Fig. 3. Demonstration of channel scattering function.

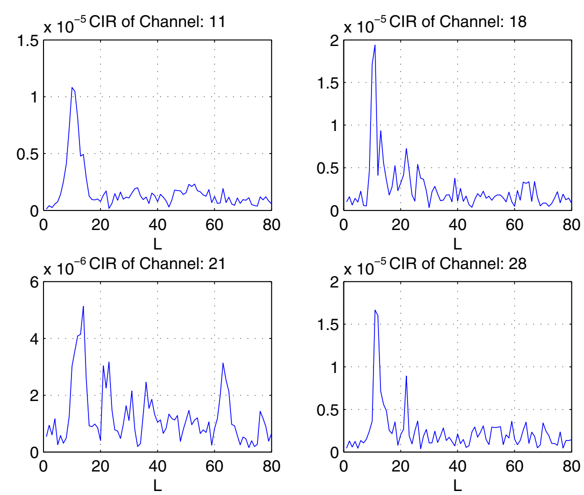

Fig. 4. MIMO channel estimation (Tx 1&2 to Rx 1&8).

two iterations are enough for achieving zero BER.

Finally, as an example of processing 2×8 MIMO block with 8PSK modulation, the soft-decision symbols at the output of the soft-decision MIMO LE and the MAP decoders are plotted in Fig. 6. We again observe the effectiveness of the iterative processing.

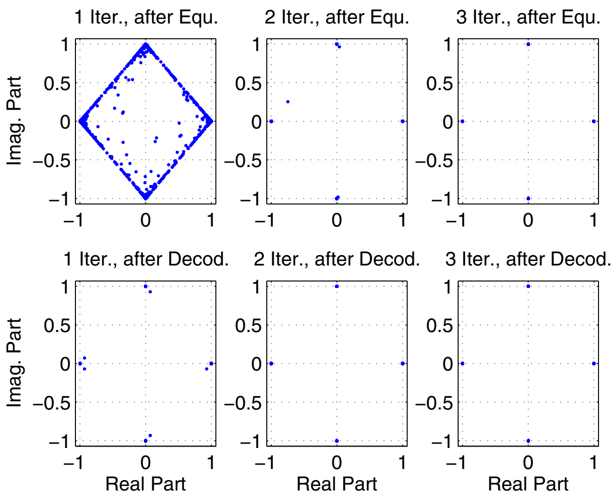

Fig. 5. Soft-decision symbols at the outputs of the equalizer and the MAP decoders (QPSK).

TABLE II
NUMBER OF ITERATIONS FOR ACHIEVING ZERO BER ($K = 1024$)

Block / Packet	1	2	3	4	5	6	7	8	9	10
1	1	1	1	1	1	1	1	1	1	2
2	2	2	2	2	2	2	2	2	2	3

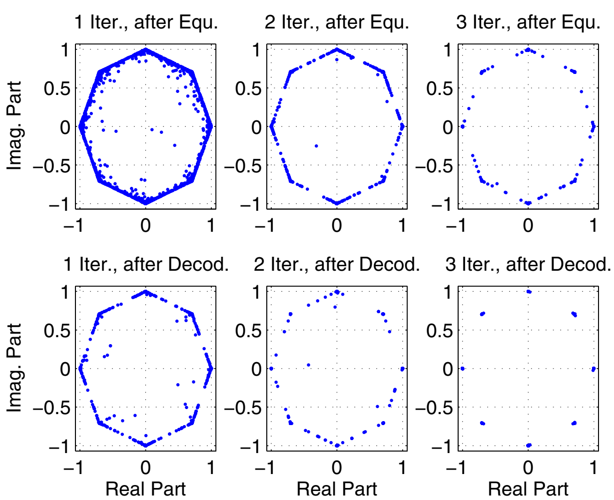

Fig. 6. Soft-decision symbols at the outputs of the equalizer and the MAP decoders (8PSK).

V. CONCLUSION

A turbo detection scheme for mobile MIMO UWA communications has been proposed in this paper. The new detection structure includes a Doppler preprocessing module aiming to compensate Doppler induced distortion in the received signal, and a MIMO turbo equalization module which provides very good detection performance with powerful iterative processing. In the MIMO turbo equalization module, a low-complexity soft-decision MIMO linear equalizer has also been proposed. The proposed turbo detection scheme has been tested by sea trial data collected during the SPACE08 experiment launched near Martha's Vineyard in 2008. The results demonstrated that the proposed detection scheme achieved excellent results with undersea experimental data.

ACKNOWLEDGMENTS

This work was supported in part by the Office of Naval Research under Grant N00014-10-1-0174 and the National Science Foundation under Grant CCF-0915846 and ECCS-0846486. We thank Dr. James Preisig and his team for conducting the SPACE08 experiment. We are also grateful to Mr. Jian Zhang for helpful discussion.

REFERENCES

[1] M. Stojanovic, J. Catipovic, and J. Proakis, "Phase-coherent digital communicaitons for underwater acoustic channels," *IEEE J. Ocean Eng.*, vol. 19, pp. 100-111, Jan. 1994.

[2] T. C. Yang, "Correlation-based decision-feedback equalizer for underwater acoustic communications," *IEEE J. Ocean Eng.*, vol. 30, pp. 865-880, Oct. 2005.

[3] B. Li, S. Zhou, M. Stojanovic, and L. Freitag, "Pilot-tone based ZP-OFDM demodulation for an underwater acoustic channel," in *Proc. MTS/IEEE Int. Oceans Conf.*, 2006.

[4] Y. R. Zheng, C. Xiao, T. C. Yang, and W. B. Yang, "Frequency-domain channel estimation and equalization for single carrier underwater acoustic communications," in *Proc. MTS/IEEE Int. Oceans Conf.*, Vancouver, 2007.

[5] J. Tao, Y. R. Zheng, C. Xiao, T. C. Yang, and W. B. Yang, "Time-domain receiver design for MIMO underwater acoustic communications," in *Proc. MTS/IEEE Int. Oceans Conf.*, Quebec City, Canada, Sept. 2008, pp. 1-6

[6] C. Douillard, M. Jezequel, C. Berrou, A. Picart, P. Didier and A. Glavieux, "Iterative correction of intersymbol interference: turbo-equalization," *Eur. Trans. Telecomm.*, vol. 6, pp. 507-511, Sept.-Oct. 1995.

[7] E. Sozer, J. Proakis, and F. Blackmon, "Iterative equalization and decoding techniques for shallow wateracoustic channels" in *Proc. MTS/IEEE Int. Oceans Conf.*, Nov. 2001, vol. 4, pp. 2201-2208

[8] F. Blackmon, E. Sozer and J. Proakis, "Iterative equalization, decoding, and soft diversity combining for underwater acoustic channels," in *Proc. MTS/IEEE Int. Oceans Conf.*, Oct. 2002, vol. 4, pp. 2425-2428

[9] S. Roy, T. M. Duman, V. McDonald, and J. Proakis, "High rate communication for underwater acoustic channels using multiple transmitters and space-time coding: receiver structures and experimental results," *IEEE J. Ocean. Eng.*, vol. 32, pp. 663-688, July 2007.

[10] J. Tao, Y. R. Zheng, C. Xiao, and T. C. Yang, "Iterative block decision feedback equalization for MIMO underwater acoustic communications," in *Proc. MTS/IEEE Int. Oceans Conf.*, Oct. 2009, pp. 1-6

[11] J. F. Sifferlen, H. C. Song, W. S. Hodgkiss, W. A. Kuperman, and J. M. Stevenson, "An iterative equalization and decoding approach for underwater acoustic communication," *IEEE J. Ocean Eng.*, vol. 33, no. 2, pp. 182-197, April 2008

[12] R. Otnes and T. H. Eggen, "Underwater acoustic communications: long-term test of turbo equalization in shallow water," *IEEE J. Ocean Eng.*, vol. 33, no. 3, pp. 321-334, July 2008

[13] J. Huang, J.-Z. Huang, C. R. Berger, S. Zhou, and P. Willett, "Iterative sparse channel estimation and decoding for underwater MIMO-OFDM," in *Proc. MTS/IEEE Int. Oceans Conf.*, Oct. 26-29, 2009.

[14] B. S. Sharif, J. Neasham, O. R. Hinton, and A. E. Adams, "A computationally efficient Doppler compensation system for underwater acoustic communications," *IEEE J. Ocean Eng.*, vol. 25, pp. 52-61, Jan. 2000.

[15] M. Tuchler, A. C. Singer, and R. Koetter, "Minimum mean square error equalization using *a priori* information," *IEEE Trans. Sig. Processing*, vol. 50, pp. 673-683, March 2002.